27th ABCM International Congress of Mechanical Engineering
December 04-08, 2023, Florianópolis-SC, Brazil

COB-2023-0951
INITIAL STUDY ON WATERJET PROPULSION FOR NAVAL VESSELS: OBTAINING PARAMETERS THROUGH CFD SIMULATIONS

Hélio Valdevieso Catarin
Arthur Sena Marques
Federal University of Santa Catarina - Estr. Dona Francisca, 8300 - Bloco U - Zona Industrial Norte, Joinville - SC, 89219-600
heliovcatarin@gmail.com**,** ar.se.marques@gmail.com

Lucas Weihmann
Federal University of Santa Catarina - Estr. Dona Francisca, 8300 - Bloco U - Zona Industrial Norte, Joinville - SC, 89219-600
lucas.weihmann@ufsc.br**.**

Andrea Piga Carboni
Federal University of Santa Catarina - Estr. Dona Francisca, 8300 - Bloco U - Zona Industrial Norte, Joinville - SC, 89219-600
andrea.piga@ufsc.br.

Abstract. *The use of alternative propulsion systems to traditional propellers is currently a highly relevant topic in naval engineering, especially in the current scenario of constant search for greater energy efficiency. One of these systems is the waterjet, widely used in jet-skis and increasingly important in small high-performance vessels, and even in larger vessels where high speeds and great maneuverability are required, as is the case with military vessels. However, despite its potential advantages, this type of propulsion is very little explored in Brazil, usually restricted to use in jet-skis and a few offshore support vessels, with few initiatives for its use in small recreational boats. Therefore, this paper presents an initial study on the topic of waterjet propulsion, with the objective of obtaining the main parameters related to its operation through CFD simulations. These parameters include the force generated by the waterjet and the moment acting on its impeller, which is used to estimate the power required for the vessel that will use the waterjet. To achieve this goal, a geometry was modeled based on the available theoretical references on the topic, and this geometry was used as a basis for study in the chosen CFD simulation software, in this case, the Simcenter STAR-CCM+. The results showed that the force generated by the waterjet is a significant parameter and the CFD simulations produced a relative error of 49.33% compared to results calculated by algebraic equations. This study highlights the importance of additional research on waterjet propulsion, as well as the potential to improve the accuracy of CFD simulations through the use of more advanced simulation techniques and refined modeling methods. Ultimately, a better understanding of the parameters related to waterjet operation will contribute to the development of more efficient and high-performance vessels.*

Keywords: *Waterjet, CFD, Simulation, Performance parameters*

1. INTRODUCTION

On certain occasions, for vessels that require special operational characteristics, traditional propeller-based propulsion systems may not be the most suitable and may encounter operational issues such as excessive cavitation. In this context, waterjet propulsion systems have been gaining market traction, not only for small high-speed vessels but also for larger ones (Carlton, 2007).

Waterjets prove to be a high-performance and efficient propulsion option, particularly when there is a need to navigate at high speeds with great maneuverability (Bulten, 2008). They are employed in smaller leisure-oriented vessels like jet boats, as well as in military vessels (Brandau, 1968) exceeding 100 meters in length, such as the Freedom and Independence-class ships of the United States Navy (Catarin, 2022). Additionally, waterjets are used in certain types of service and search and rescue vessels.

According to Carlton (2007), the operating principle of this type of propulsion system is essentially based on an internal pump, consisting of an impeller, stator, and nozzle assembly. It draws water through ducts connected to an opening at the bottom of the vessel's hull and subsequently expels it backwards at high velocities by adding energy to the water. The system also includes a steering device, as indicated in Figure 1. Centrifugal pumps are typically used for waterjet systems with lower specific speeds, while mixed flow, axial flow, and inducer pumps are also employed when higher speeds are required.

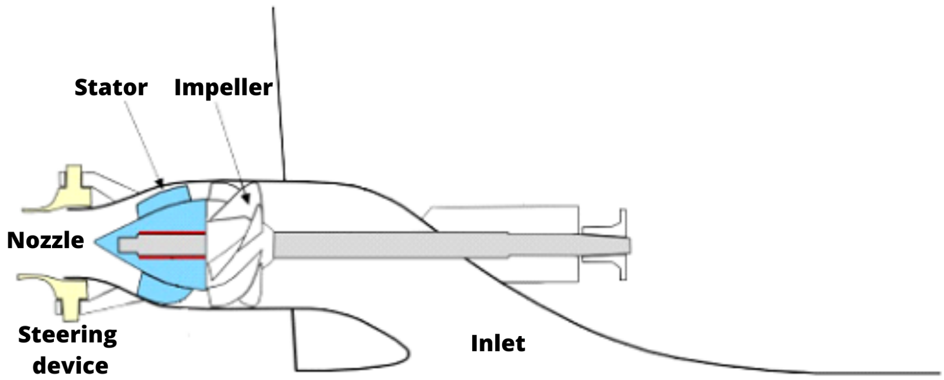

Figure 1. Main components of a waterjet (adapted from Borrett e Birkinshaw (2007)).

Given the great potential of this type of propulsion for vessels, which is still largely unexplored in Brazil, an initial study was conducted based on waterjet propulsion systems. In this context, computational fluid dynamics (CFD) simulations proved to be a good starting point, as they allow for the analysis of more complex geometries, such as the waterjet. CFD simulation provides performance predictions of its components even before the construction and testing of prototypes, highlighting its significant potential for use in the industry as a whole (Fox, 2010).

Therefore, the methodology to be employed initially consists of gathering relevant previous studies on the subject, followed by the construction of a geometry based on the analysis of available literature for the purpose of testing and adjusting the necessary parameters for computational fluid dynamics simulation using the STAR CCM+ software.

After this initial testing phase, the focus will be on studying the operation of the waterjet and obtaining relevant data for its application, such as the maximum thrust that the device can provide and the moment generated by the flow passing over the impeller blades. This parameter can be used to estimate the power required for the device, where the input parameters for these simulations are the impeller's rotation and the vessel's velocity.

This way, a brief theoretical foundation (Chapter 2) will be presented next, with the aim of introducing the main concepts and equations related to waterjets, followed by the description of the methodology adopted for this work (Chapter 3). Then, in Chapter 4, the development of the simulations will be presented. With the simulations duly presented, the results are discussed next in Chapter 5, and finally, the conclusions and suggestions for future work are presented in Chapter 6.

2. THEORETICAL FOUNDATION

2.1 Characteristic Speeds

According Bulten (2006) a complete waterjet system can be divided into four characteristic velocities: the ship velocity (V_{ship}), which is considered constant in steady-state conditions, the inlet velocity (V_{in}), which is described by a velocity profile due to the interaction with the vessel's bottom, the pump velocity (V_{pump}), and finally, the outlet velocity (V_{out}). The location of these velocities within the waterjet system can be seen in Figure 2.

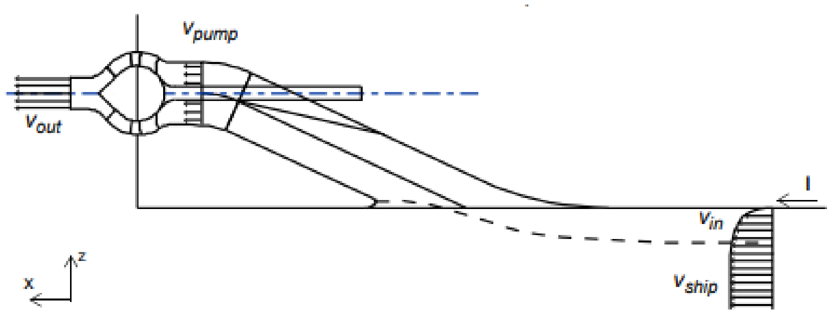

Figure 2. Characteristic speeds of a waterjet (Bulten, 2006).

One way to understand the influence of these velocities on the waterjet is through the calculation of the Inlet Velocity Ratio (IVR), as in Eq. (1), which relates V_{pump} to the average inlet velocity V_{in} previously mentioned, and is limited to an operational range from 0 to approximately 2.5. Above this range, there is a high likelihood of encountering cavitation issues at the waterjet's inlet pipe, which can sometimes be mitigated by an appropriate inlet geometry (Arif, 2021).

$$IVR = \frac{V_{ship}}{V_{pump}} \tag{1}$$

where IVR represents the Inlet Velocity Ratio, the forces acting on the waterjet itself and $T_{wj,hull}$ represents the region of the hull surrounding the waterjet inlet, as shown in Figure 3 (Arif, 2021).

2.2 Thrust Generated by a Waterjet

As described by Bulten (2006), the accelerated water flow through the jet installation generates a reactive force on the vessel's structure, which propels the vessel forward.

To determine this thrust, it is necessary to establish a control volume. According to Bulten (2006), the control volume should encompass the jet's ducting on one side and the solid region of the hull on the other, as depicted in Figure 3. This enables the analysis of the forces involved during the system's operation.

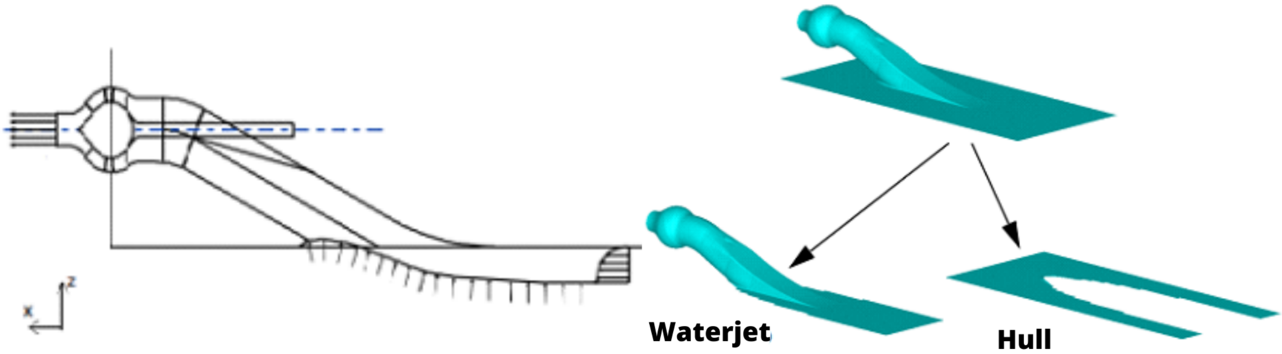

Figure 3. Control volume for a waterjet (adapted from Bulten, 2006).

Thus, the thrust T_{wj} in the x-direction (according to the coordinate system in Figure 3) generated by a complete waterjet installation is calculated through the balance of forces acting on it, represented in this work by the sum of two force components, as shown in Eq. (2).

$$T_{wj} = T_{wj,tube} + T_{wj,hull} \tag{2}$$

where $T_{wj,tube}$ represents the forces acting on the waterjet itself and $T_{wj,hull}$ represents the region of the hull surrounding the waterjet inlet, as shown in Figure 3 (Bulten, 2006).

The contribution of pressure cannot be quantified analytically since its distribution is unknown, making its calculation complex even for numerical methods. However, this force component, as well as the $T_{wj,hull}$ component, are small compared to the primary $T_{wj,tube}$ component, allowing for the simplification of Eq. (2) to Eq. (3), which provides a simplified way to estimate the thrust of a waterjet (Jiao et al., 2019).

$$T_{wj} = \rho . Q\left(V_{out} - V_{in}\right) \tag{3}$$

where T_{wj} represents the thrust generated by a waterjet, density ρ of the water, the volumetric flow rate Q passing through the system and the velocity difference V_{in} and V_{out} (Jiao et al., 2019).

3. METHODOLOGY

The methodology followed for the execution of this work is presented. Initially, a literature survey was conducted on the topic at hand, which highlighted the relatively small amount of previous works related to CFD simulation of waterjets and the difficulty in accessing them.

The chosen software for the simulations was Simcenter STAR-CCM+ due to its great versatility, allowing the application of a large number of physical models. Compared to other similar software, it also has a relatively good amount of available material on its functioning and a more user-friendly interface for initiating CFD simulations. It is worth mentioning that it is available in the Naval Simulation Laboratory and the Subaquatic Technology Laboratory (LASUB) at CTJ, UFSC.

The simulation of a rotating fan was performed in order to validate the methodology. After validating the obtained results with those available in Siemens (2021), the necessary knowledge for configuring rotational motions in the STAR-CCM+ software was developed.

Subsequently, a geometry was constructed in Rhinoceros software based on the geometry used by Bulten (2006) and served as the initial testing platform for the simulations built in the STAR-CCM+ software. Initially, only the inlet tube of a waterjet without a pump was simulated, allowing for a qualitative analysis of the results by comparing them to the results presented by Bulten (2006). For this, the same inlet and outlet velocities were used because, in this case, without a pump, an outlet velocity must be established at the end of the jet tube.

After this comparison, the complete jet geometry was employed in the simulations, enabling the acquisition of performance parameters of the constructed geometry, such as thrust and moment acting on the impeller, as well as visualization of various other quantities using the scene creation feature of STAR-CCM+. Among the knowledge developed in these simulations, mesh generation and selection of the physical models to be used in the simulation of a waterjet are noteworthy.

Since this geometry was only based on the one used by Bulten (2006) and presented significant differences, especially in the impeller and the absence of a stator, its results could not be quantitatively validated, only compared to the result obtained through Eq. (2). Some qualitative analyses could also be performed.

The input parameters used for the simulations were the same as those used by Bulten (2006) in his works. Table 1 shows the values of velocity and impeller rotation that were used.

Table 1. Simulation input parameters

Variable	**Partial geometry**	**Complete geometry**
V_{ship}, m/s	8	8
Impeller rotation speed, rpm	-	1920

4. DEVELOPMENT

This chapter aims to present the geometries used for the construction of the domains, as well as the discussions related to the simulations themselves.

4.1 Geometry

The geometry used in this work was entirely constructed using the 3D modeling software Rhinoceros and represents the internal region through which the fluid flows in a scale model of a waterjet tested experimentally in a cavitation tunnel, as described by Bulten (2006).

It is worth noting that an important component of this type of propulsion, the stator, was omitted due to the lack of information in the published work regarding its geometry. The stator plays a significant role in the waterjet as stated by Carlton (2007), as its main function is to correct the flow after it has passed through the impeller, removing the jet swirl and also acting as a support for the tube.

The domain used refers to the region below the waterjet, essentially a parallelepiped composed of water, which, in this case, represents a section of the cavitation tunnel used in the experiments conducted by Bulten (2006), along with the waterjet's tubing. The tunnel is bounded by walls on the top, bottom, and sides, while its cross-section represents the water inlet and outlet.

Two different domains were used for the initial geometry: the first one being simplified, containing only the tunnel section, the inlet tube, and the shaft, while the second one being more comprehensive, including the complete waterjet tubing, including the outlet tube. The first domain was used for some quantitative analyses that will be presented in the following chapters, while the second (more comprehensive) was used for calculating the performance parameters of the initial geometry.

The dimensions of the tunnel region used consist of a cross-section of 600 millimeters by 600 millimeters, with a length of 1509.09 millimeters, as shown in Figure 4. These dimensions were also based on the geometries used by

Bulten (2006), and in the absence of other reference sources, and after conducting some tests by varying these dimensions, it was observed that increasing them would not bring significant changes in the simulation results.

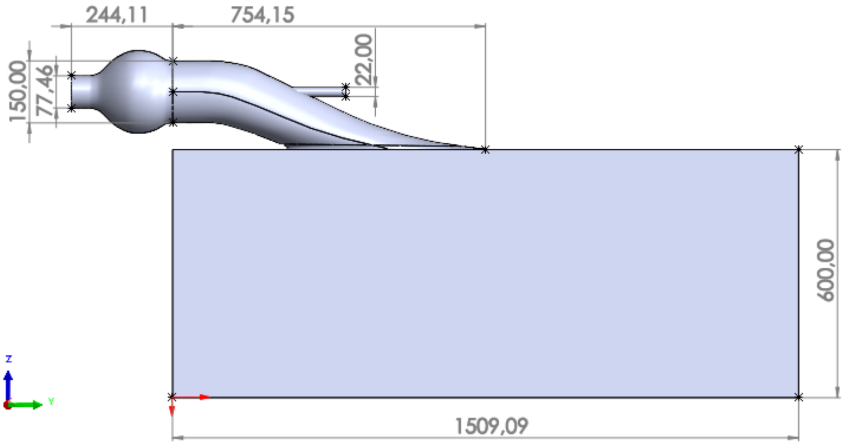

Figure 4. Domains used in simulations.

The tubing of the initial geometry was divided into two parts: the inlet tube or intake, which corresponds to the domain region located just above the tunnel section and represents the water inlet region in the propulsion system, and the pressure tube, which covers the impeller and the jet outlet, increasing the velocity of the outgoing flow by reducing the diameter of the tube section, as depicted in Figure 5. The shape of this region resembles that of a mixed flow pump and characterizes the pump of this waterjet system.

The rotational domain defines the region where rotational motion of the impeller will be applied in the simulation. In this case, due to the impeller's shape, it is represented by a simple sphere, highlighted in blue in Figure 5. It is important to note that the impeller is contained within this domain.

All these geometries were constructed using Rhinoceros software, based on the geometry employed by Bulten (2006), where the contours and dimensions provided by Bulten were utilized in this study.

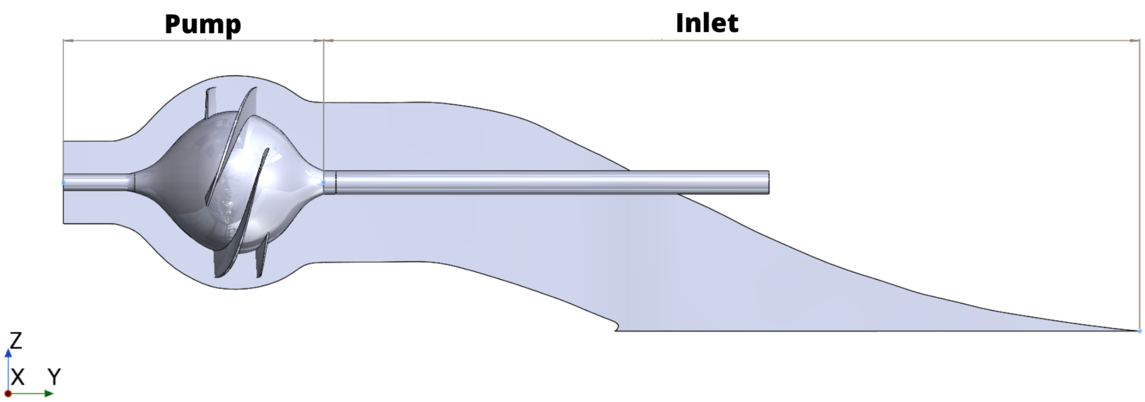

Figure 5. Piping, rotational and impeller-shaft assembly from geometry.

As it is a much more complex geometry and due to the lack of information in the main work used as a reference, a generic impeller from a waterjet was used, as shown in Figure 5. Since the purpose of this initial simulation was to develop and adapt this propulsion system in the STAR-CCM+ software, the only modifications made to the impeller were its main dimensions to suit the specific requirements of this study.

Passing through the inlet tube, there is the impeller shaft, which connects the motor to the impeller located inside the waterjet. The diameter of the shaft used was 22 millimeters. The shaft-impeller assembly can be seen in Figure 5.

4.2 Simulations

As mentioned earlier, the software used for the CFD simulations was Simcenter STAR-CCM+.

The purpose of the simulations performed in this work was to use the aforementioned software to obtain the thrust generated by the waterjet and the moment acting on its impeller. This parameter is crucial for estimating the required power of the vessel's propulsion system. In addition to the geometry representing the flow path in a waterjet propulsion system, the necessary inputs to the software also include the impeller rotation speed and the ship velocity, V_{ship}.

Therefore, this chapter will present the key aspects of the simulations. It is worth noting that two simulations with distinct domains were conducted, as described in the previous chapter: one focused solely on analyzing the waterjet inlet tube, and the other involving the complete initial waterjet configuration.

4.2.1 Motion Tool

According to Siemens (2021), the STAR-CCM+ software provides different approaches for handling elements that are subject to some form of motion. Among them, two methods stand out for simulating the component discussed here: the Moving Reference Frame (MRF) and the Rigid Body Motion (RBM), each with distinct operational characteristics, configuration options, and computational performance requirements.

In the Moving Reference Frame approach, also known as frozen impeller, a region is defined to move with respect to a specified reference frame, highlighting the significance of the previously discussed rotational geometry. By default, STAR-CCM+ provides a stationary reference frame, but it also allows for the creation of moving reference frames that can rotate and translate. These frames are used to simulate rigid rotations and translations of a region without moving the mesh vertices, effectively transforming a transient problem into a static problem in the moving reference frame (Siemens, 2021).

On the other hand, in the Rigid Body Motion approach, the mesh vertices are allowed to move during a transient analysis, while the component undergoing this motion remains undeformed. This method enables the modeling of problems where a region rotates about a fixed axis, translates along a fixed direction, or combines both types of motion (Siemens, 2021).

It is important to note that a simulation using Rigid Body Motion requires significantly more computational processing and, in some cases, may take longer to reach convergent solutions compared to a simulation using the Moving Reference Frame. However, Rigid Body Motion can provide more accurate solutions that better represent reality (Siemens, 2021).

Given the computational challenges involved, this study opted for using the Moving Reference Frame method to simulate the impeller rotation, although some tests involving Rigid Body Motion were also performed.

4.2.2 Definition of Physical Models

The employed software features a wide range of models and physical methods necessary for simulating various scenarios, including single-phase and multiphase fluid flows, heat transfer, turbulence, solid stress, fluid-body dynamic interaction, aeroacoustics, among others. Thus, its versatility in solving different engineering problems stands out.

These models play a crucial role in the simulation as they determine the formulation and solution approach applied by the software. The correct selection of physical models can be the difference between a convergent or non-convergent simulation and whether it is consistent with reality (Siemens, 2021).

Some of the basic models used include liquid (water), three-dimensional, turbulent, and constant density. In addition to these, the segregated fluid model was also employed, which solves the conservation equations of mass and momentum sequentially. It is a good alternative for incompressible or slightly compressible flows, requiring slightly fewer computational resources (Siemens, 2021).

In relation to turbulence, the k-Epsilon model was employed (Luo et al., 2021). This two-equation model solves transport equations for turbulent kinetic energy and turbulent dissipation rate to calculate turbulent viscosity. This is a well-established model, having been refined over several years, and is today the predominant choice for industrial applications (Siemens, 2021).

As mentioned earlier, the Moving Reference Frame requires a steady-state simulation, while Rigid Body Motion is implicitly unsteady. In this work, the Segregated Flow Solver with a SIMPLE pressure-velocity coupling algorithm was used.

In addition to these, other models are automatically selected based on the choice of one or another model. For example, the Reynolds-averaged Navier-Stokes (RANS) averaging for the equations of motion (Arif, 2021), solution interpolation, among others.

4.2.3 Definition of Regions

The previously described geometries and components are used solely to define the faces, edges, and vertices that make up the surfaces of the model. The simulation domain, where the mesh is generated and the physics of the problem are solved, is defined using regions, boundaries, and interfaces.

However, to create the regions, the mesh subtraction tool was used for geometry preparation. This operation removes parts of one geometry from another, which was particularly helpful in subtracting components such as the impeller, shaft, stator, and the rotational itself from within the domain. This operation was performed twice, resulting in two geometry parts ready to be converted into regions. The first part corresponds to the domain itself, from which the shaft and rotational geometries were removed, and the second part corresponds to the rotational component, from which the impeller geometry was subtracted.

It is important to note that the domain represents the path through which the fluid flows, and when a specific geometry is removed from its interior, that area will no longer be traversed by the fluid, thus characterizing the internal components of the waterjet.

Once the regions were constructed, it became possible to configure and assign the physical function to each face that composes the waterjet geometry. In this way, three types of boundaries were used: inlet velocity, outlet pressure, and wall, as shown in Figure 6, where the faces corresponding to each type of boundary are highlighted in red, orange, and gray, respectively (Gong et al., 2022).

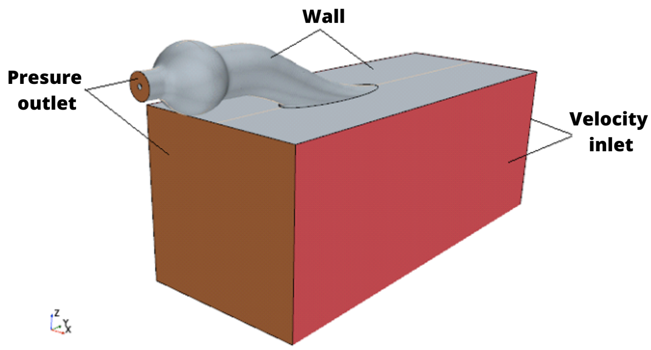

Figure 6. Full geometry regions.

The inlet velocity boundaries represent the known velocity flow entering the system, in this case, the parameter V_{ship}, while also establishing the direction of vessel navigation. This type of inlet boundary is compatible with the outlet pressure boundary used in the flow exit regions (Siemens, 2021).

Lastly, the wall boundary represents an impermeable surface where, for viscous flows, the no-slip condition is applied by default. This means that the fluid adheres to and moves with the same velocity as the wall. In other words, for a stationary wall, the fluid will have a velocity of zero relative to it (Siemens, 2021).

4.2.4 Definition of Mesh

The employed cell model was Trimmed Cell, which utilizes hexahedral cells, and then cuts or trims the mesh according to the part's surface. The Prism Layer model was also used, which is responsible for generating layers of orthogonal prismatic cells near the part's surface or boundaries, playing a crucial role in improving the flow solution's accuracy (SIEMENS, 2021). In addition to these, the Surface Remesher and Automatic Surface Repair models were used, which are responsible for enhancing mesh quality and correcting geometry issues during mesh generation, respectively. Thus, the mesh used in the final simulation consisted of a total of 1,75 millions of cells with a Base Size of 17,5 millimeters.

5. RESULTS AND DISCUSSIONS

5.1 Scenes

Through the pressure coefficient plots, it is possible to perform a qualitative analysis of the partial geometry inlet tube simulation for an IVR of 2.03, by comparing the results obtained in this CFD simulation with the results presented by Bulten (2006). This comparison is shown in Figure 7, where it can be observed that, in general, the pressure coefficient exhibits similar behavior in both images, with particular emphasis on the regions circled in red and blue.

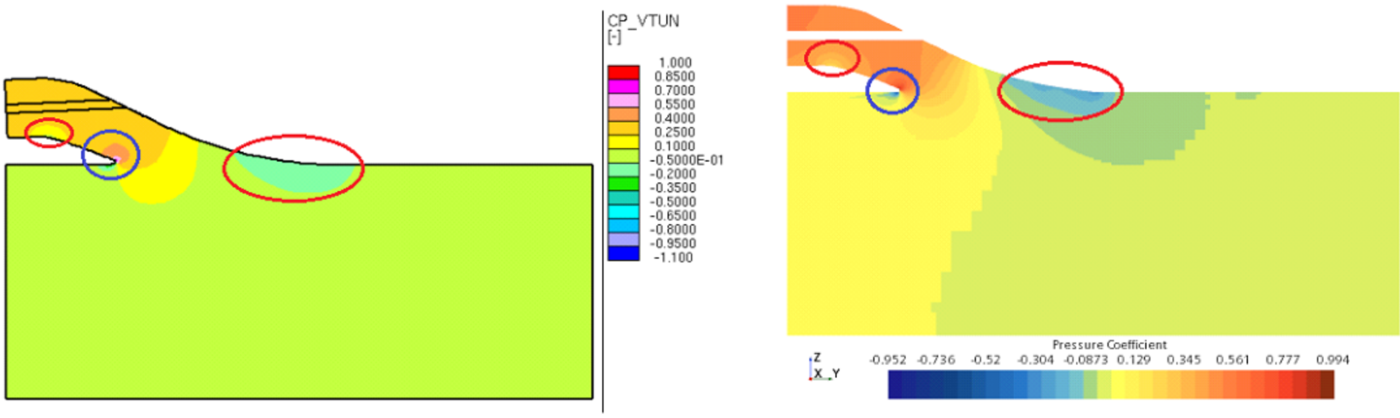

Figure 7. Pressure coefficient presented by Bulten (2006) (left) and pressure coefficient obtained in this work via CFD simulation (right).

The highlighted region in blue in Figure 7 deserves special attention, as stated by Bulten (2006). Waterjets operating with higher IVRs (above 2) typically exhibit similar behavior, namely, a low pressure coefficient just below the jet inlet at the bottom region of the vessel (dark blue region highlighted in Figure 7), and a high pressure coefficient just above the inlet (reddish region highlighted in blue in Figure 7).

In addition to these, velocity profiles in the jet flow direction were also analyzed. These profiles allow the identification of low-efficiency points in the waterjet geometries, enabling optimization for more efficient geometries. Thus, Figure 8 presents the scalar velocity profile in the flow direction on the central plane for the complete geometry.

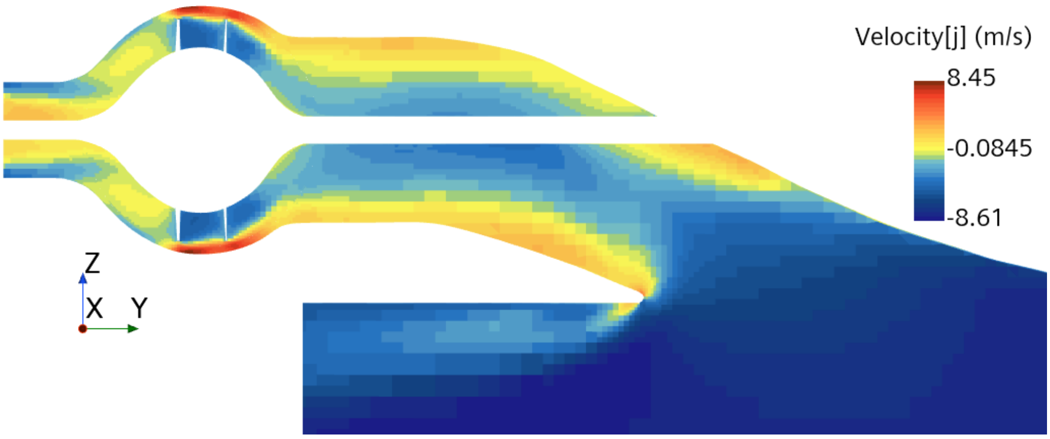

Figure 8. Speed for full geometry.

5.2 Thrust

Regarding the thrust, Figure 9 displays the graph of the obtained results for this crucial performance analysis parameter of a waterjet as a function of the number of iterations for the complete geometry.

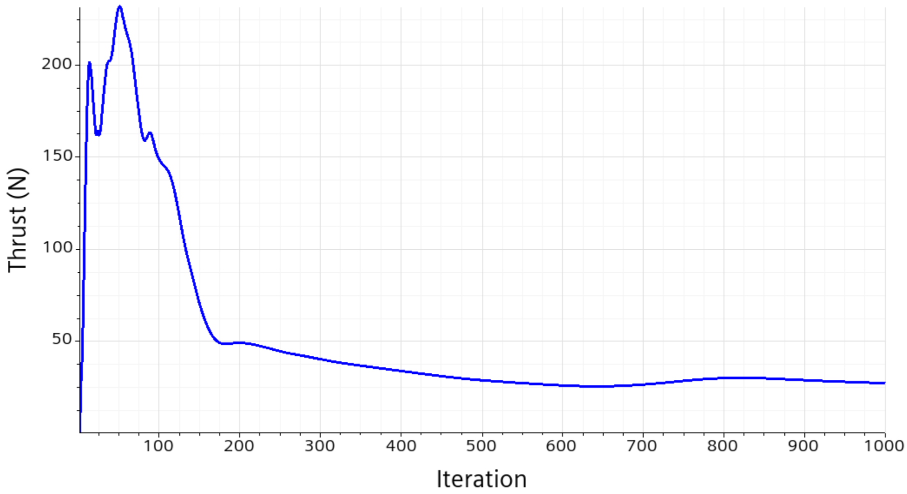

Figure 9. Thrust generated by complete geometry.

Analyzing the graph in Figure 9, it can be observed that the number of iterations was sufficiently high for the simulation result to converge, reaching a thrust value of 26.90 newtons in its last iteration. Considering the mass flow rate value presented in the previous section and the inlet and outlet areas of the initial jet geometry, obtained from the Rhinoceros software, using Eq. (2), a value of 53.09 newtons was found. Therefore, comparing the values obtained from the simulation and the equation, the observed relative error is 49.33%.

This difference can be attributed to the various considerations the software makes for thrust calculation compared to those used in applying Eq. (2). Specifically, the software may take into account a different inlet velocity than the one considered in the algebraic equation.

Furthermore, it is worth noting that due to significant differences in the geometry constructed in this work compared to the geometry used by Bulten (2006), along with the fact that Bulten presents numerical results in the form of dimensionless relative values using average values, making an efficient and accurate comparison difficult.

5.3 Impeller moment

This quantity can be used to calculate the estimated power required for the propulsion system of a waterjet-powered vessel, highlighting the importance of its estimation. Thus, Figure 10 shows the moment graph as a function of simulation iterations, where a moment of -12.82 Nm was found. The axis of rotation for this moment is the impeller shaft of the waterjet pump.

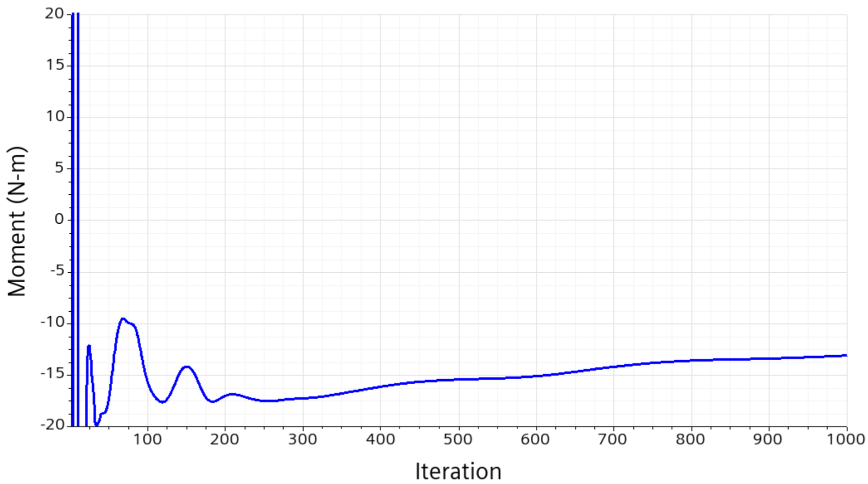

Figure 10. Moment on the impeller of the complete geometry.

6. CONCLUSION AND SUGGESTIONS FOR FUTURE WORK

In light of all the findings presented in this study, it is demonstrated the significant importance and effectiveness of using Computational Fluid Dynamics (CFD) simulations in solving engineering problems, especially in cases where there is a limited amount of available research material or situations involving complex geometries that are difficult to represent using traditional analytical methods.

Thus, the use of simulations proves to be an important tool that aids in the development of an engineering project, bridging the gap between the initial design phases and the construction of test prototypes. It allows for the analysis of the performance of components with more complex geometries, such as the waterjet, without the need for their physical construction and testing. This does not invalidate or replace the use of prototype testing but enables a greater number of design iterations to be analyzed before the actual construction of the component.

This translates into potential resource savings, where only components that have been validated through simulations are actually built and tested.

Regarding the obtained results, the qualitative analysis carried out using the pressure coefficients of the partial geometry inlet tube provides an indication that the models used in the simulations are suitable for the proposed analyses. The same can be said for the comparison between the thrust results obtained through simulation and the application of Eq. (2).

However, these results are not sufficient for a quantitative validation of the thrust and moment values found in the simulation, primarily due to significant approximations made in obtaining the necessary inlet and outlet velocities for the application of Eq. (2), as well as the necessary considerations for constructing this equation. A potential alternative for validating the results obtained in this work could involve conducting experiments, either through scaled-down tests in test tanks, as presented by Bulten (2006), or through tests on actual vessels.

As a suggestion for future work, a more in-depth analysis of the required mesh quality could be performed to make better use of the available computational resources. Additionally, a study utilizing simulations with the employment of rigid body motion capabilities in the STAR-CCM+ software, for a possible performance comparison with the frame of reference motion method, could also be conducted.

Lastly, as mentioned above, comparing the simulation results with experimental results would be ideal for validating the simulations, thereby ensuring that the physics of the problem at hand have been accurately represented.

7. REFERENCES

Arif, B.; Ayuningtyas, H.. Performance analysis of waterjet propulsion on an unmanned surface vehicle model. Journal Of Applied Engineering Science, [S.L.], v. 19, n. 4, p. 886-895, 2021. Centre for Evaluation in Education and Science (CEON/CEES). http://dx.doi.org/10.5937/jaes0-29942.

Borrett, D.; Birkinshaw, A.. Use of Main Drive Waterjets as Azimuth Thrusters. Christchurch: Dynamic Positioning Committee, 2007.

Brandau, J. H. (1968). Performance of Waterjet Propulsion Systems- A Review of the State-of-the-Art. Journal of Hydronautics, 2(2), 61–73. https://doi. org/10.2514/3.62775

Bulten, N. W. H.. Numerical Analysis of a Waterjet Propulsion System. 2006. Dissertação (Master's thesis, Graduate Program in Mechanical Engineering) – Technische Universiteit Eindhoven, Eindhoven, 2006.

Bulten, N. (2008). A Breakthrough in Waterjet Propulsion Systems. Doha International Maritime Defence Exhibition and Conference DIMDEX. https:// doi.org/10.1.1.552.3994

Carlton, J. Marine propellers and propulsion. 2. ed. Burlington: Butteworth-Heinemann, 2007.

Catarin, H. V.. Simulação em cfd de um hidrojato comercial. 2022. 78 f. TCC (Graduação) - Curso de Engenharia Naval, Universidade Federal de Santa Catarina, Joinville, 2022.

Fox, R. W.; Pritchard, P. J.; Mcdonald, A. T. Introdução à mecânica dos fluidos. 7. ed. Rio de Janeiro: Ltc, 2011.

Gong, Jie; Wu, Z.; Ding, J.; Jiang, J.; Zhang, Z.. Numerical analysis of propulsion performance of a waterjet-propelled vehicle in steady drift. Ocean Engineering, [S.L.], v. 266, p. 113136, dez. 2022. Elsevier BV. http://dx.doi.org/10.1016/j.oceaneng.2022.113136.

Jiao, W., Cheng, L., Zhang, D., Zhang, B., Su, Y., & Wang, C. (2019). Optimal Design of Inlet Passage for Waterjet Propulsion System Based on Flow and Geometric Parameters. Advances in Materials Science and Engineering, 2019. https://doi. org/10.1155/2019/2320981

Luo, X.; Li, Q.; Zhang, Z.; Zhang, J.. Research on the underwater noise radiation of high pressure waterjet propulsion. Ocean Engineering, [S.L.], v. 219, p. 108438, jan. 2021. Elsevier BV. http://dx.doi.org/10.1016/j.oceaneng.2020.108438.

SIEMENS DIGITAL INDUSTRIES SOFTWARE. Simcenter STAR-CCM+ User Guide, version 2021.2.

8. RESPONSIBILITY NOTICE

The authors are the only responsible for the printed material included in this paper.